X-ray Structure Analysis of a Thermoplastic Polyimide

Kenji Okuyama,* Hisashi Sakaitani, and Hiroyuki Arikawa

Faculty of Technology, Tokyo University of Agriculture and Technology, Koganei, Tokyo 184, Japan

Received June 17, 1992; Revised Manuscript Received August 31, 1992

ABSTRACT: The molecular and crystal structure of a new thermoplastic polyimide, poly[(5,7-dihydro-1,3,5,7-tetraoxobenzo[1,2-*c*:4,5-*c'*]dipyrrole-2,6(1*H*,3*H*)-diyl)-1,3-phenyleneoxy[1,1'-biphenyl]-4,4'-diyloxy-1,3-phenylene] (TPI), was analyzed by means of an X-ray diffraction method and a linked-atom least-squares method. From diffraction patterns of oriented films of this polyimide, unit cell dimensions were determined to be a = 7.89 Å, b = 6.29 Å, c(fiber axis) = 25.11 Å, and β = 90.0°. The space group was $P2_1$. The unit cell contains two polymer chains with a 1/1-helical symmetry. One chain is located at the center of the four equivalent polymer chains. There are no interactions between neighboring molecules but van der Waals interactions. Aromatic ring planes tilt about 30–40° to the neighboring planes due to the short atomic interactions between directly-linked aromatic moieties. Because of the mutual compensation of two bending parts of the polymer chain, the overall molecular conformation is quite straight, which gives TPI mechanical strength and stability. On the other hand, the four degrees of freedom of TPI decrease the melting temperature to 382 °C, which enables the melt processing of this polyimide.

Introduction

Good thermal stability of polymer is achieved by introduction of rigid aromatic rings and heterocyclic moieties into the polymer backbone. However, the rigidity of polymers thus obtained causes the high glass transition temperature (T_g) and the high melting temperature (T_m), which makes polymers extremely difficult to melt for their processing. For example, the polyimides Vespel and Kapton, produced by du Pont, are known for outstanding mechanical properties and excellent thermal stability. However, since the melting temperatures of these polyimides are higher than their decomposition temperatures, it is impossible to use melt processing, which is very common for almost all plastic resins. In the practical point of view, therefore, it is important to lower the melting temperature to some extent without losing thermal stability.

Recently, a new thermoplastic polyimide, poly[(5,7-dihydro-1,3,5,7-tetraoxobenzo[1,2,-*c*:4,5-*c'*]dipyrrole-2,6-(1*H*,3*H*)-diyl)-1,3-phenyleneoxy[1,1'-biphenyl]-4,4'-diyloxy-1,3-phenylene] (TPI), was synthesized by Mitsui Toatsu Chemicals, Inc. Since the melting temperature of this polymer is 382 °C, it melts without polymer decomposition and it is thermally stable up to its deformation temperature of 236 °C.

In addition to poor cyrstallinity, the number of X-ray diffraction spots is usually not enough for precise structure analysis of polyimides. Hence, there has been no report of structural details for polyimides. Although the quality of X-ray diffraction data from TPI is similar to those from other polyimides, we tried to analyze the precise molecular and crystal structure of TPI to get a better understanding of the physical properties of this polymer. For accomplishing this analysis we used a linked-atom least-squares method together with X-ray diffraction data.

Materials and Methods

(a) Materials. Sample polymer TPI, was kindly donated by Mitsui Toatsu Chemicals, Inc. The chemical formula is shown in Figure 1a, together with atomic numbering and the seven variable dihedral angles. The weight-average molecular weight of this polymer was about 2.5×10^4 by small-angle light scattering[1] and the molecular weight distribution M_w/M_n was 2.9 by GPC.[1]

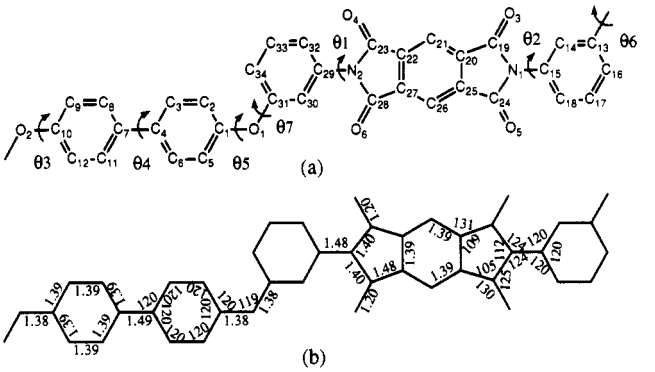

Figure 1. (a) Chemical structure of a repeating unit of TPI and dihedral angles varied in the refinement calculations. (b) Bond lengths (Å) and bond angles (deg) used in the molecular model building and refinement calculations. Every phenylene ring was treated as an equilateral hexagon. Bond angles at ether oxygens were fixed to 119° in the first stage of analysis. However, they were varied in the final refinement calculations.

The glass transition temperature (T_g) of this polymer was 244 °C by DSC measurement. The original films were obtained by crystallizing the amorphous molded sheet at about 320 °C after heating above the melting temperature (382 °C). To get oriented specimens, the film was subsequently drawn four times at 290 °C and annealed at 290 °C for 30 min with fixed ends. The unoriented specimen film from which X-ray intensities were measured was obtained by annealing at 300 °C for 2 h.

The density of the specimen was measured by a flotation method with a mixture of *n*-hexane and carbon tetrachloride.

(b) X-ray Diffraction. X-ray diffraction patterns were recorded with a cylindrical camera using nickel-filtered Cu Kα radiation from an X-ray generator (ROTA FLEX RU-200, Rigaku). The interplanar spacings were measured from the X-ray diffraction patterns using a STOE film-measuring device. Since there were many meridional reflections compared with nonmeridional ones, the intensities were not measured from the fiber diffraction pattern of the oriented specimen, but from the pattern of the unoriented specimen (film thickness, 0.2 mm) to include meridional reflections in an intensity data set. Further, the reflections below the observational threshold were also included in the data for the refinement calculations. That is, unobserved reflections with spacings longer than those of the observed ones were assumed to have one-third of an intensity for the observational threshold. These unobserved reflection data were used only when the magnitude of the calculated structure amplitude became larger than that of the estimated structure amplitude

0024-9297/92/2225-7261$03.00/0

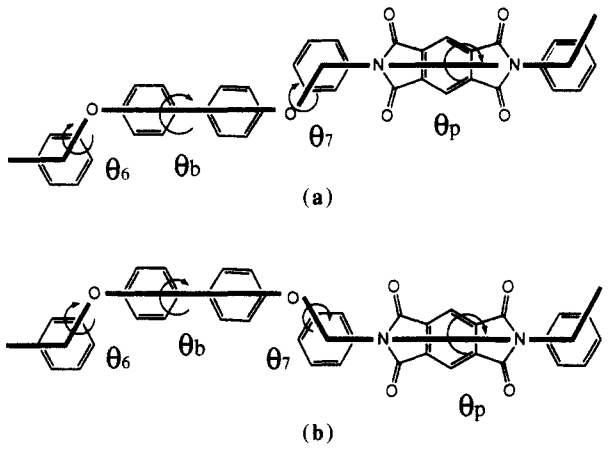

Figure 2. Two nonsymmetrical molecular models of TPI: (a) trans model; (b) cis model. Solid lines denote virtual bonds of TPI.

($|F_c| > |F_o|$) during the refinement calculations. The intensity (I_o) for the unoriented specimen was estimated by visual comparison with a standard intensity scale. Since every diffraction ring was spread to some extent, all reflections whose spacings were inside of the corresponding line width were considered to overlap each other. These intensities were corrected for the Lorentz and polarization factors (Lp) by using the following equation:

$$F_o = (I_o/Lp)^{1/2} \qquad 1/Lp = 2 \sin 2\theta \sin \theta/(1 + \cos^2 2\theta) \qquad (1)$$

where F_o denotes the observed structure amplitude, θ denotes the Bragg angle of the reflection. The data were not corrected for absorption in this study.

(c) Molecular Model Building. Molecular models having the appropriate helical symmetry and fiber repeating period were generated using a linked-atom description[2] with fixed bond lengths and angles. These values are shown in Figure 1b. A total of 18 hydrogen atoms were linked to the corresponding carbon atoms with a bond length of 1.08 Å and a bond angle of 120°. The bond angle at the ether oxygen was fixed at 119° that was found in the single-crystal structure of 3,3',4,4'-tetrachlorodiphenyl ether.[3] At the last stage of analysis, however, this angle was included in the refinement variables. As shown in the following section, the molecular structure of TPI had a 1/1-helical symmetry in which one chemical repeating unit was contained in a fiber repeating period. Although there are seven conformational angles in a chemical repeating unit (Figure 1a), the pair θ_1 and θ_2 and the three angles θ_3, θ_4, and θ_5 are mutually related by the para-linked pyromellitimide and the para-linked biphenyl moiety, respectively. These relationships are formulated as $\theta_p = \theta_1 + \theta_2$ and $\theta_b = \theta_3 + \theta_4 + \theta_5$. As a result, the helical conformation is defined only by four dihedral angles, θ_6, θ_7, θ_b, and θ_p. The space of the helical conformation for TPI with the appropriate helical parameters (unit height, h = 25.11 Å, and unit twist, θ = 360°) was investigated by the numerical calculation method,[4] which revealed only two possible models. One is a cis model in which $\theta_7 = \theta_6 \approx 180°$ and $\theta_b = \theta_p \approx 0°$, and the other is a trans model in which $\theta_7 = \theta_6 \approx 180°$ and $\theta_b = \theta_p \approx 180°$ (Figure 2).

To fix the orientations of two para-linked benzene moieties and the pyromellitimide moiety, the values of dihedral angles θ_1, θ_3, and θ_4 have to be given. Planes like a benzene and pyromellitimide usually cannot lie on the same plane due to the steric hindrance, when they connect directly. As a starting molecular conformation, therefore, one of the values of 45, 90, and 135° was systematically assigned to θ_1, θ_3, and θ_4, which generated a total of 27 (=3^3) molecular conformation models for each of the cis and trans models.

In addition to the above conformational models, the following three symmetrical conformational models were also considered. The first is the center of inversion model in which there are inversion centers at the center of the pyromellitimide and biphenyl moieties. To ensure this symmetry, constraining conditions of $\theta_p = \theta_b = 180°$, $\theta_4 = 0°$, and $\theta_7 = -\theta_6$ were applied. To build an appropriate molecular conformation, θ_6 and θ_7 must be in the vicinity of 180°. Therefore, this inversion model is a special case of the above trans model, where the additional condition of $\theta_4 = 0°$ is demanded. The steric hindrance between directly-linked benzene rings will be discussed in a later section. The second is the mirror model in which there are mirror symmetries at the center of the pyromellitimide and biphenyl moieties perpendicular to the helical axis. To ensure the mirror symmetry, the constraining conditions of $\theta_p = \theta_b = 0$, $\theta_4 = 0$, and $\theta_7 = \theta_6 = 180°$ were applied. Since the molecular conformation with such values for dihedral angles could not have the observed unit height (h = 25.11 Å) and unit twis (θ = 360°), the mirror model was excluded from further considerations. The third is the 2-fold model in which there are 2-fold symmetries at the center of the pyromellitimide and normal to its plane and at the center of biphenyl moiety and parallel to the bisector of adjacent benzene planes. In this case, the applied constraining conditions were $\theta_p = 2\theta_1 = 2\theta_2$, $\theta_4 = 180°$, $\theta_5 = \theta_3$, and $\theta_7 = \theta_6$.

Table I
Observed (d_o) and Calculated (d_c) Spacings Together with Intensities of TPI[a]

d_o	d_c	h	k	l	intensity
		Equator			
5.05	4.92	±1	1	0	vs
3.93	3.94	2	0	0	vs
3.36	3.41	±2	1	0	m
3.10	3.15	0	2	0	m
2.90	2.92	±1	2	0	m
2.40	2.42	±3	1	0	w
2.00	2.02	±3	2	0	w
		First Layer			
25.46	25.11	0	0	1	vs
6.13	6.10	0	1	1	m
		Second Layer			
4.66	4.58	±1	1	2	m
		Third Layer			
8.50	8.37	0	0	3	w
5.72	5.74	±1	0	3	vw
4.30	4.24	±1	1	3	w
3.08	3.10	±2	1	3	vw
		Fourth Layer			
6.23	6.27	0	0	4	s
		Fifth Layer			
5.02	5.02	0	0	5	m
2.56	2.53	±1	2	5	vw
		Sixth Layer			
4.22	4.18	0	0	6	s
		Seventh Layer			
3.55	3.58	0	0	7	m
		Eighth Layer			
2.33	2.29	±2	1	8	vw

[a] Intensities are denoted by vs (very strong), s (strong), m (medium), w (weak), and vw (very weak).

(d) Packing Models and Their Refinement. To obtain the appropriate packing models in a unit cell, the polymer chain position (u) along the a-axis and the azimuthal angle (μ) have to be determined. Since the diffraction spot composed of (±1,1,0) reflections had a very strong intensity (Table I), one chain was located at the center of four other equivalent chains. Because of the space group $P2_1$, these chains are related by crystallographic 2_1 symmetry along the b-axis running at $u = 0$ and $1/2$. Therefore, at first, one of the four corner molecules was located at $u = 0.25$. On the other hand, the value v along the b-axis can be chosen arbitrarily in the space group $P2_1$. The azimuthal angle of the polymer chain, μ, was systematically changed by 30-deg intervals from 0 to 150° for each molecular model. A total of 162 (=27 × 6) packing models were generated for each of the cis and trans models in the case of the nonsymmetrical molecules. These models were examined in terms of the agreement between calculated and observed structure amplitudes and intramolecular short contacts between nonbonded atoms. Since the calculated structure amplitudes of equatorial reflections were independent

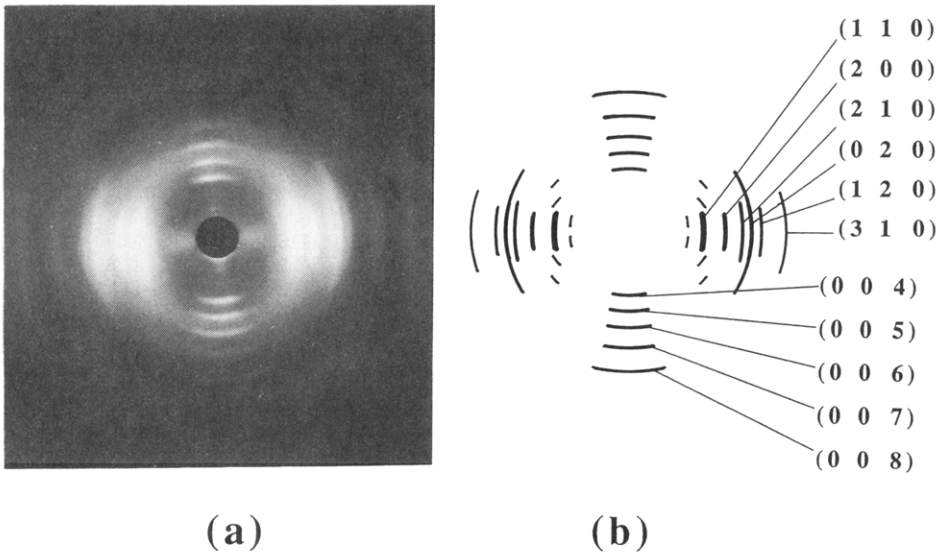

Figure 3. (a) X-ray diffraction pattern of TPI taken by a cylindrical camera and (b) its schematic illustration. This diffraction pattern was used for obtaining lattice constants and indexing of the reflections. For intensity measurement, the diffraction from the unoriented specimen was used.

of the translational parameter (w) of the polymer chain along the fiber (c) axis, only the equatorial reflections were used as X-ray intensity data at the first stage of analysis. These were 7 observed reflections and 4 reflections below the observational threshold. The models in which the calculated structure amplitudes were in good agreement with the observed ones (R less than 0.30) were further refined with $\theta_1, \theta_2, \theta_3, \theta_4, \theta_5, \mu$, and u as variable parameters. There were 31 trans-type models and 12 cis-type models that passed the R-factor test on the basis of equatorial reflections only. Most of these initial models refined to one of 6 distinct trans-type models or one of 3 distinct cis-type models. These models had R values less than 0.15. Then, the translational parameter (w) was examined for each of the above 9 models, by changing w stepwisely by increments of 0.05 from 0.0 to 0.5. All the intensity data from the unoriented specimen and nonbonded atomic interactions between intra- and intermolecules were used in these calculations.

For the symmetric molecular models, a similar procedure was applied in constructing the packing models. After refinement against equatorial reflections, the 2-fold model was excluded because of the poor agreement between observed and calculated structure amplitudes.

At each stage in the modeling and refinement of the structure, we sought to minimize the quantity Ω in the following least-squares fashion.[2]

$$\Omega = \sum w_m(|F_{om}| - |F_{cm}|)^2 + S\sum \epsilon_j + \sum \lambda_h G_h \qquad (2)$$

The first term ensures the optimum agreement between the observed (F_{om}) and the calculated (F_{cm}) X-ray structure amplitudes. In this study, we used $w_m = 1.0$ for all reflections. The second ensures the optimization of noncovalent interatomic interactions. The third imposes, by the method of Lagrange undetermined multipliers, the exact constraints we have chosen. The agreement between observed and calculated structure amplitudes was evaluated by R and R_w, which were defined by

$$R = \sum ||F_o| - |F_c|| / \sum |F_o| \qquad R_w = \sum (|F_o| - |F_c|)^2 / \sum F_o^2 \qquad (3)$$

Atomic scattering factors for calculating structure factors were obtained using the method and values given in ref 5. Computations were done on the ACOS 1000 computer at the Information Processing Center, Tokyo University of Agriculture and Technology.

Structure Determination

(a) Crystal Data. Figure 3 shows an X-ray fiber diffraction pattern from the oriented TPI specimen and its schematic illustration. A total of 20 observed diffractions in the fiber diagram was indexed by the rectangular unit cell with the dimensions $a = 7.89$, $b = 6.29$ Å, and c(fiber axis) = 25.11 Å. Measured and calculated spacings for observed reflections are listed in Table I, together with the corresponding Miller indices. Assuming that the unit cell contains two chemical repeating units, the calculated density of 1.47 g cm^{-3} agrees with the observed value (1.38 g cm^{-3}). Since the extended length of a chemical repeating unit (25.6 Å) is more than that of the fiber repeating unit (25.11 Å), two packing models are possible. One is the two-chain model in which the unit cell contains two polymer chains with a 1/1-helical symmetry; the other is the one-chain model in which the unit cell contains only one polymer chain with a 2/1-helical symmetry. However, the very strong (001) reflection and other (00l) reflections on the odd layer lines ($l = 3, 5, 7$) supported the 1/1-helical structure as a polymer conformation. Furthermore, the very strong (±1,1,0) reflection also suggested the two-chain model in which one chain is located at the center of the other four equivalent chains.

Because of the small number of reflections, the space group could not be determined definitely at the first stage of analysis. Then, we performed the structure analysis for the space group $P1$, which revealed that there was a relation of 2_1 symmetry between two polymer chains in a unit cell. In this paper, only the result for the space group $P2_1$ will be shown.

(b) Molecular and Crystal Structure. In the case of a nonsymmetrical molecular model, totally, 162 packing models for each of the cis and trans models were examined in terms of 11 equatorial reflections and intramolecular atomic contacts. The 43 candidates (31 for the trans model and 12 for the cis model) with R values less than 0.30 were refined with variable parameters of θ_1, θ_2, θ_3, θ_4, θ_5, μ, u, and scale factor, which resulted in the convergence to 6 distinct trans-type models and 3 distinct cis-type models. After the translational parameter (w) was examined, each of these 9 models was refined further against all intensity data and interaction data between nonbonded atoms. As a result, four trans-type models remained plausible, whereas none of the cis-type models remained. By looking at these four models (A, A′, B, and B′ in Table II) carefully, it was found that two of them were essentially the same packing model, since A′ and B′ models were very similar to the A and B models, respectively. That is, for example,

Table II
Four Nonsymmetrical Models of TPI and Their Refined Conformations, Together with the Refined Inversion Model[a]

	model A			model B			
	A	A′	refined model	B	B′	refined model	inversion model
θ_1	47.8	47.9	44.4	55.6	55.3	52.9	39.8
θ_2	132.2	132.1	135.7	124.4	124.7	127.1	140.2
θ_3	66.0	109.6	75.3	58.8	102.6	64.5	108.4
θ_4	43.0	−41.7	45.1	43.6	−39.0	36.0	(0.0)
θ_5	70.9	112.1	59.7	77.6	116.5	79.5	71.6
θ_6	(152.9)	(152.9)	145.1	(152.9)	(152.9)	144.5	148.3
θ_7	(−152.9)	(−152.9)	−145.1	(−152.9)	(−152.9)	−144.5	−148.3
τ(COC)	(119.0)	(119.0)	126.4	(119.0)	(119.0)	127.2	123.0
ξ_x	(131.2)	(131.2)	145.7	(131.2)	(131.2)	147.1	139.5
ξ_y	(72.6)	(72.6)	72.6	(72.6)	(72.6)	72.6	72.6
ξ_z	(54.4)	(54.4)	45.1	(54.4)	(54.4)	43.4	48.8
μ	42.0	42.2	51.1	53.6	53.7	65.4	44.9
u	0.231	0.269	0.233	0.244	0.257	0.247	0.241
w	0.064	0.437	0.059	0.153	0.347	0.161	0.017
scale factor	3.911	3.913	4.541	3.935	3.941	4.740	4.597
B_{iso}	(10.0)	(10.0)	3.3	(10.0)	(10.0)	2.3	4.2
R	0.240	0.238	0.203	0.217	0.222	0.203	0.238
R_w	0.243	0.243	0.200	0.274	0.276	0.240	0.271
R(excl unobs)	0.177	0.178	0.163	0.142	0.145	0.142	0.197
R_w(excl unobs)	0.199	0.199	0.174	0.173	0.174	0.168	0.235
Ω			4.44×10^3			6.14×10^3	5.05×10^3

[a] The values in parentheses were fixed during the calculations.

if the opposite chain direction was chosen for the model A, the values of conformational angles of this model will be $\theta_1 = 132.2$, $\theta_2 = 47.8$, $\theta_3 = 70.9$, $\theta_4 = 43.0$, $\theta_5 = 66.0$, $\theta_6 = -152.9$, and $\theta_7 = 152.9°$. Then, the mirror image of this conformation will be $\theta_1 = -132.2$, $\theta_2 = -47.8$, $\theta_3 = -70.9$, $\theta_4 = -43.0$, $\theta_5 = -66.0$, $\theta_6 = 152.9$, and $\theta_7 = -152.9°$. When the definition of the conformational angles in the para-linked biphenyl and pyromellitimide moieties is changed, the values of θ_1, θ_2, θ_3, and θ_5 can be changed to $\theta_1 + 180°$, $\theta_2 + 180°$, $\theta_3 + 180°$, and $\theta_5 + 180°$, respectively. Finally, we obtain the conformation with $\theta_1 = 47.8$, $\theta_2 = 132.2$, $\theta_3 = 109.1$, $\theta_4 = -43.0$, $\theta_5 = 114.0$, $\theta_6 = 152.9$, and $\theta_7 = -152.9$, which is very similar to model A. Therefore, the number of packing models was reduced to two, models A and B. Although these two models also have similar molecular conformations, models A and B were submitted to further refinement calculations.

In the final calculations, the constraining conditions $\theta_1 + \theta_2 = \theta_p$ and $\theta_3 + \theta_4 + \theta_5 = \theta_b$ were released so that the refinement parameters were θ_1, θ_2, θ_3, θ_4, θ_5, θ_6, θ_7, ξ_x, ξ_y, ξ_z, μ, u, w, scale factor, and overall isotropic thermal parameter (B_{iso}). In addition to these, bond angles $\angle C_1O_1C_{31}$ and $\angle C_{10}O_2C_{13}$ were also included in the variables, since the angle of ether oxygen was known to be in the fairly wide range. The refined structure of model A (Table II) showed a good agreement between observed and calculated structure amplitudes ($R = 0.203$ and $R_w = 0.200$, or $R = 0.163$ and $R_w = 0.174$ for the reflections excluding those below the threshold). On the other hand, the refined model B showed similar R values ($R = 0.203$ and $R_w = 0.240$, or $R = 0.142$ and $R_w = 0.168$ for the reflections excluding those below the threshold). Even after refinement calculations, the molecular conformations of models A and B are very similar to each other. The main difference comes from the chain translational parameter (w). Because of this difference, some short contacts between adjacent molecules were observed in the structure of model B, for example, 2.89 ($C_5 \cdots C_{34}$), 2.95 ($C_{18} \cdots C_{24}$), and 2.66 Å ($C_{14} \cdots O_3$). In the case of model A, no such short contacts were observed between adjacent molecules. Furthermore, the value of Ω of model A was significantly better than that of model B. Because of these facts we concluded that model A was more reasonable than model B, even though R and R_w values of model A were slightly higher than the corresponding values of model B.

Table III
Fractional Atomic Coordinates of TPI

atom	x	y	z
C_1	0.100 45	−0.017 56	−0.074 68
C_2	0.269 98	0.018 04	−0.062 54
C_3	0.322 29	0.024 96	−0.009 71
C_4	0.205 07	−0.003 71	0.030 98
C_5	−0.016 77	−0.046 24	−0.033 98
C_6	0.035 54	−0.039 31	0.018 85
C_7	0.261 13	0.003 71	0.087 62
C_8	0.370 25	0.163 35	0.104 64
C_9	0.422 55	0.170 28	0.157 47
C_{10}	0.365 75	0.017 56	0.193 28
C_{11}	0.204 33	−0.149 00	0.123 43
C_{12}	0.256 64	−0.142 08	0.176 26
C_{13}	0.361 04	0.163 71	0.284 29
C_{14}	0.345 29	0.096 17	0.336 76
C_{15}	0.288 25	0.236 44	0.375 60
C_{16}	0.319 75	0.371 52	0.270 65
C_{17}	0.262 70	0.511 80	0.309 49
C_{18}	0.246 95	0.444 26	0.361 96
C_{19}	0.325 61	0.282 86	0.475 52
C_{20}	0.283 59	0.149 95	0.522 33
C_{21}	0.307 68	0.185 09	0.576 46
C_{22}	0.256 31	0.032 96	0.613 22
C_{23}	0.266 61	0.029 89	0.672 07
C_{24}	0.199 59	−0.029 88	0.446 53
C_{25}	0.209 89	−0.032 96	0.505 38
C_{26}	0.158 52	−0.185 09	0.542 14
C_{27}	0.182 61	−0.149 95	0.596 27
C_{28}	0.140 59	−0.282 86	0.643 08
C_{29}	0.177 95	−0.236 44	0.743 00
C_{30}	0.120 91	−0.096 16	0.781 84
C_{31}	0.105 15	−0.163 71	0.834 31
C_{32}	0.219 25	−0.444 26	0.756 64
C_{33}	0.203 49	−0.511 80	0.809 11
C_{34}	0.146 45	−0.371 52	0.847 95
O_1	0.048 52	−0.024 44	−0.127 13
O_2	0.417 68	0.024 44	0.245 73
O_3	0.391 30	0.454 69	0.473 28
O_4	0.322 55	0.159 93	0.702 30
O_5	0.143 64	−0.159 92	0.416 30
O_6	0.074 89	−0.454 69	0.645 32
N_1	0.271 47	0.164 53	0.431 47
N_2	0.194 73	−0.164 53	0.687 13

Table IV
Observed (F_o) and Calculated (F_c) Structure Amplitudes of TPI[a]

refl no.	h	k	l	F_c	F_o	refl no.	h	k	l	F_c	F_o
1	0	0	1	41.5	25.6	33	±3	0	1	13.7	(58.5)
2	1	0	0	36.1	(18.4)	34	±2	1	6	39.7	(58.7)
3	±1	0	1	44.2	(19.2)	35	±3	0	2	19.2	(59.6)
4	0	0	2	2.0	(11.4)	36	0	1	9	66.1	(60.3)
5	0	0	3	4.0	(17.3)	37	±1	2	5	34.1	(60.8)
6	±1	0	2	41.0	(22.6)	38	0	2	6	23.6	(61.2)
7	0	0	4			39	0	0	10	6.7	(61.3)
	0	1	1	102.8	57.8	40	±3	0	3	59.8	(61.3)
8	±1	0	3			41	±2	2	0		
	0	1	2	66.8	53.1		±2	0	8		
9	0	1	3				±2	2	1		
	0	0	5				±2	1	7		
	±1	1	0				±3	1	0		
	±1	0	4	164.1	185.0		±1	1	9		
10	±1	1	1				±3	0	4		
	±1	1	2	155.6	165.1		±3	1	1		
11	0	1	4				±2	2	2		
	±1	1	3				±1	2	6	149.0	164.1
	±1	0	5			42	±1	0	10	24.9	(64.8)
	0	0	6	91.3	98.6	43	±3	1	2	108.4	(65.1)
12	2	0	0			44	0	2	7	60.4	(65.6)
	0	1	5			45	±2	2	3	42.6	(65.8)
	±2	0	1			46	0	1	10		
	±1	1	4	238.8	230.3		±3	1	3		
13	±2	0	2	25.0	(39.4)		±3	0	5		
14	±1	0	6	26.4	(40.2)		±2	2	4		
15	0	0	7				±2	1	8	92.9	130.5
	±2	0	3			47	0	0	11	7.7	(68.4)
	±1	1	5	56.6	99.1	48	±2	0	9	56.6	(68.5)
16	0	1	6	37.5	(42.7)	49	±1	2	7	56.7	(68.9)
17	±2	1	0			50	±3	1	4	28.0	(69.0)
	±2	0	4			51	±1	1	10	53.0	(70.0)
	±2	1	1			52	±3	0	6	21.8	(70.4)
	±1	0	7	209.8	205.1	53	0	2	8	17.9	(70.5)
18	±2	1	2			54	±2	2	5	41.5	(71.0)
	±1	1	6			55	±1	0	11	28.0	(71.7)
	0	2	0			56	±3	1	5	48.5	(71.9)
	0	0	8	186.1	229.1	57	0	1	11		
19	0	2	1	71.7	(48.1)		±2	1	9		
20	0	1	7	23.7	(48.3)		±1	2	8		
21	±2	1	3				±2	2	6		
	±2	0	5				±3	0	7		
	0	2	2				±2	0	10		
	±2	1	4				±3	1	6		
	0	2	3				0	3	0	111.2	130.5
	±1	2	0			58	0	0	12	10.5	(75.7)
	±1	0	8			59	0	3	1	20.2	(75.7)
	±1	2	1			60	0	2	9	28.9	(75.9)
	±1	1	7	163.6	152.7	61	±1	1	11	43.6	(76.7)
22	±2	0	6	16.8	(52.8)	62	0	3	2	23.5	(76.7)
23	±1	2	2	50.9	(53.3)	63	0	3	3		
24	0	2	4	39.5	(54.0)		±2	2	7		
25	0	1	8	26.8	(54.6)		±1	3	0		
26	0	0	9				±1	0	12		
	±2	1	5				±1	3	1		
	±1	2	3	61.0	89.1		±3	2	0		
27	0	2	5	30.8	(57.3)		±1	2	9		
28	±2	0	7	6.7	(57.6)		±3	0	8		
29	±1	2	4	37.9	(57.7)		±3	2	1		
30	±1	1	8	43.5	(57.8)		±3	1	7		
31	3	0	0	13.3	(58.2)		±2	1	10		
32	±1	0	9	16.4	(58.2)		±1	3	2	177.4	147.3

[a] Reflections with F_o values in parentheses are unobserved ones. These values were obtained from one-third of the observational threshold.

In the case of symmetrical molecular models, similar calculations were carried out. After several refinement cycles for equatorial reflections, the 2-fold model was excluded from further consideration because of the poor agreement between observed and calculated structure amplitudes. On the other hand, one of the inversion models showed fairly good agreement (R = 0.238 and R_w = 0.271, or R = 0.197 and R_w = 0.235 for the reflections excluding those below the threshold; see Table II). The molecular conformation is very similar to that of model A. The essential difference comes from θ_4, which was fixed at 0° for the inversion model, whereas θ_4 was varied in model A. Some short contacts between adjacent molecules were observed in the inversion model, such as 2.57 ($C_{24}\cdots O_6$), 2.87 ($C_{22}\cdots O_3$), and 2.61 Å ($O_5\cdots O_6$). Finally, we chose model A as the structure of TPI by the reason mentioned in the following section. The final atomic coordinates of the chemical repeating unit of model A are listed in Table III. Observed and calculated structure amplitudes are listed in Table IV.

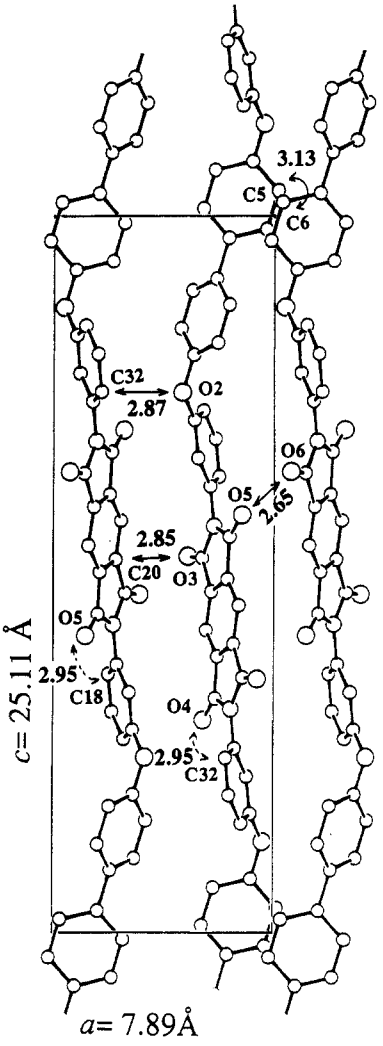

Figure 4. Packing structure of TPI viewed along the *b*-axis (ORTEP drawing[10]). Some short contacts between neighboring molecules are shown.

Results and Discussion

(a) Molecular Conformation. The obtained molecular conformation is shown in Figure 4. In the chemical repeating unit, there are two types of bending parts (Figure 1). One is *m*-benzene and the other is the ether linkage part. However, the overall molecular conformation is quite straight (Figure 4) due to the mutual compensation of these bending parts. The conformational angles that determine the molecular structure, θ_6, θ_7, θ_p, and θ_b, are 145.1, -145.1, 180.0 (=44.35° + 135.65°), and 180.0° (=75.285° + 45.06° + 59.655°), respectively. Deviations from the trans conformation are seen in θ_6 and θ_7 by 34.9°. This makes the fiber repeating period somewhat shorter than that of the fully-extended structure.

After final refinement calculations, the bond angles at the ether oxygen, $\angle C_1O_1C_{31}$ and $\angle C_{10}O_2C_{13}$, were changed from the initial value of 119 to 126.4°. The obtained angle is quite larger than that found in the low molecular weight compound.[3] Since this kind of rather wide oxygen bond angle was found in the structures of poly(*p*-phenylene oxide)[6] (124°) and poly(2,6-diphenyl-*p*-phenylene oxide)[7] (127°), this may become larger in the aromatic polymer crystal, comparing with those in the low molecular weight compounds. On the contrary, in the case of aliphatic polyoxide, the corresponding bond angle was found to be rather small (112°).[8,9]

The mutual orientations of the adjacent aromatic planes were 44.4 (θ_1), 135.7 (θ_2), and 45.1° (θ_4). These values were quite reasonable since the simple calculation between directly connected aromatic rings showed that the deviation from the planar conformation (cis or trans) must be more than 30°, to avoid short atomic contacts. In fact, this angle for biphenyl was reported to be 42° in the gas phase.[11] Furthermore, these angles in several biphenyl derivatives also deviate by about 30–40° from the planar conformation. These were 28.7, 35.5, and 32.3° in the structures of 4-biphenylcarboxylic acid,[12] 31.0° in 3-chlorobiphenyl-4-carbonitrile,[13] and 46° in 4-biphenyl thioketone,[14] respectively. However, it was also reported that, in the cases of modifications of 4-hydroxybiphenyl[15] and biphenyl itself,[16] the torsion angles were almost 0°. In these crystals biphenyl planes stack regularly and make a well-ordered structure. The intermolecular interactions in a well-ordered structure seem to stabilize the biphenyl conformation with the intramolecular energy maximum ($\theta_4 \approx 0°$). In the cases of most biphenyl derivatives,[12-14] however, this kind of strong interaction of biphenyl moieties was not observed in their packing structures. In this study, the symmetrical molecular models in which the biphenyl moiety had a planar conformation were considered at the first stage of analysis. One of such models gave a fairly good *R* value and showed a very similar conformation compared to the best model for nonsymmetrical cases (Table II). As shown in the following section, however, there is no such strong interaction between biphenyls like those in 4-hydroxybiphenyl and biphenyl itself. Therefore, we concluded that the biphenyl moiety of TPI would not take a planar conformation similar to that of biphenyl itself.

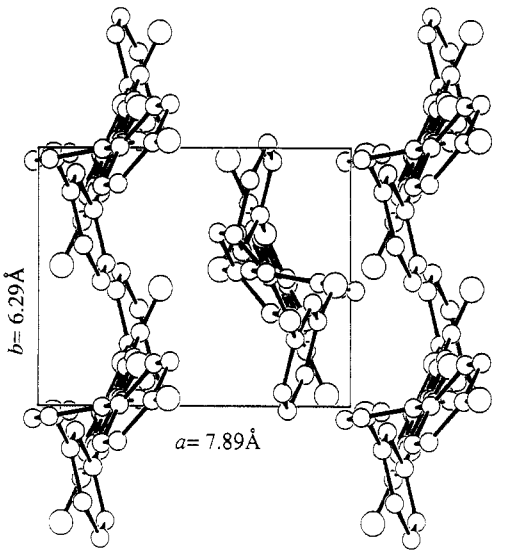

Figure 5. Packing structure of TPI viewed along the *c*(fiber)-axis.

Some short contacts between directly-linked aromatic moieties were found. These are 3.02 ($O_4\cdots C_{30}$, $O_6\cdots C_{32}$, $O_5\cdots C_{14}$, and $O_3\cdots C_{18}$), 3.02 ($C_3\cdots C_8$ and $C_6\cdots C_{11}$), and 2.98 Å ($C_1\cdots C_{34}$ and $C_{10}\cdots C_{16}$). The first interactions are those between a *m*-phenyl ring and a pyromellitimide, the second are between phenylene rings in the biphenyl moieties, and the last are between a *m*-phenyl ring and a biphenyl moiety.

(b) Packing Structure. Figure 5 shows the packing structure projected along the *c*(fiber)-axis. The unit cell contains two polymer chains related by 2_1 symmetry along the *b*-axis. Therefore, one polymer chain is surrounded by four adjacent chains with the opposite direction. In spite of the different chain direction, these two chains look very similar, as shown in Figure 4, since TPI has an inversion center in a chemical structure. There are no

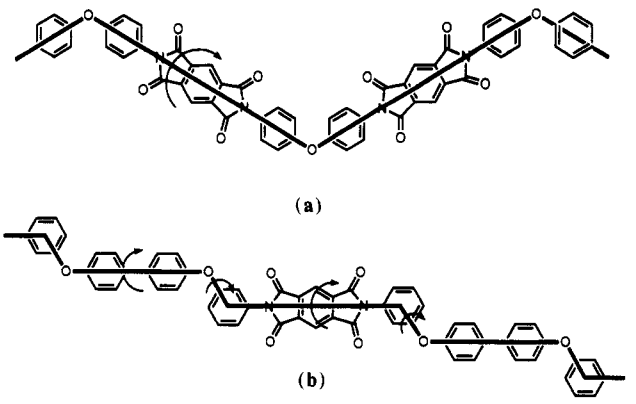

Figure 6. Comparison of rotational freedom of TPI with that of Vespel. Vespel has only one rotational freedom in a chemical repeating unit (a), while TPI has four (b).

other interactions between molecules but van der Waals interactions. Fairly short atomic contacts are observed between neighboring molecules. These are 2.65 (O_5···O_6), 2.85 (O_3···C_{20}), 2.87 (O_2···C_{32}), 2.95 (O_4···C_{32} and O_5···C_{18}), and 3.13 Å (C_5···C_6). Together with short contacts between directly-linked aromatic moieties, these atomic interactions ristrict rotational angles around virtual bonds of *p*-benzene and pyromellitimide.

In conclusion, newly synthesized TPI has four bending parts at meta-linked benzene moieties and ether oxygen parts in a main chain, which makes the degree of freedom of this molecule equal to 4 (Figure 6b), that is, there are four rotational angles in a chemical repeating unit. In the case of Vespel, such a bending part is at the ether oxygen part. Therefore, the degree of freedom in the chemical repeating unit is only 1 (Figure 6a). In comparison with the case of Vespel, this difference of degree of freedom lowers the melting temperature of TPI, which enables the melt processing of this polyimide. On the other hand, even though TPI has four bending parts, the overall chain conformation is almost straight and very close to the fully-extended conformation. Furthermore, to avoid short interactions between directly-linked aromatic moieties, these aromatic planes tilt about 40° to each other, which makes the surface of the molecule uneven. The mechanical stability of TPI might be attributed to these structural features.

References and Notes

(1) Tanaka, K.; Yukawa, Y.; Oosuga, H.; Ohoshima, K.; Ooe, H.; Nakamura, M.; Simegi, K. *Polym. Prepr., Jpn.* **1989**, *38*, 3341–3343.
(2) Smith, P. J. C.; Arnott, S. *Acta Crystallogr.* **1977**, *A34*, 3–11.
(3) Singh, P.; Mckinney, J. D. *Acta Crystallogr.* **1980**, *B36*, 210–212.
(4) Go, N.; Okuyama, K. *Macromolecules* **1976**, *9*, 867–868.
(5) *International Tables for Crystallography*; Ibers, J. A., Hamilton, W. C., Eds.; Kynoch Press: Birmingham, England, 1974; Vol. 4, pp 71–147.
(6) Boon, J.; Magre, E. P. *Makromol. Chem.* **1969**, *126*, 130–138.
(7) Boon, J.; Magre, E. P. *Makromol. Chem.* **1970**, *136*, 267–280.
(8) Tadokoro, H.; Takahashi, Y.; Chatani, Y.; Kakida, H. *Makromol. Chem.* **1967**, *109*, 96–111.
(9) Uchida, T.; Tadokoro, H. *J. Polym. Sci., Phys. Ed.* **1967**, *5*, 63–81.
(10) Johnson, C. K. Report ORNL-5138; Oak Ridge National Laboratory: Oak Ridge, TN, 1976.
(11) Almenningen, A.; Bastiansen, O. *Skr.—K. Nor. Vidensk. Selsk.* **1958**, *4*, 1–16.
(12) Brock, C. P.; Blackburn, J. R.; Haller, K. *Acta Crystallogr.* **1984**, *B40*, 493–498.
(13) Sutherland, H. H.; Rawas, A. *Acta Crystallogr.* **1984**, *C40*, 830–832.
(14) Arjunnan, P.; Ramamurthy, V.; Venkatesan, K. *Acta Crystallogr.* **1984**, *C40*, 556–558.
(15) Brock, C. P.; Haller, K. L. *J. Phys. Chem.* **1984**, *88*, 3570–3574.
(16) Charbonneau, G. P.; Delugeard, Y. *Acta Crystallogr.* **1977**, *B33*, 1586–1588.